Small-angle neutron scattering study of a magnetically inhomogeneous amorphous alloy with reentrant behavior

R. García Calderón, L. Fernández Barquín, S. N. Kaul,* and J. C. Gómez Sal
Departamento CITIMAC, F. Ciencias, Universidad de Cantabria, 39005 Santander, Spain

Pedro Gorria
Departamento de Física, Universidad de Oviedo, 33007 Oviedo, Spain

J. S. Pedersen†
Condensed Matter Physics and Chemistry Department, Risoe National Laboratory, DK-4000, Roskilde, Denmark

R. K. Heenan
ISIS Facility, Rutherford Appleton Laboratory, Chilton, Didcot, Oxon OX11 0QX, United Kingdom
(Received 21 June 2004; revised manuscript received 2 November 2004; published 19 April 2005)

Small-angle neutron scattering (SANS) measurements have been performed on an archetypal reentrant amorphous ferromagnet $Fe_{91}Zr_9$ over the Q range $0.003\ \text{Å}^{-1} < Q < 0.2\ \text{Å}^{-1}$ and temperatures between 10 and 300 K at fixed values of magnetic field $H=0$, 0.26, 0.5, and 4 T. Contrast matching experiments have also been carried out at room temperature before and after immersing the ribbons in deuterium oxide. The results of these experiments demonstrate that the surface effects tend to be important only for $Q < 0.006\ \text{Å}^{-1}$. Application of a field $H=4$ T much larger than that corresponding to the technical saturation of magnetization allows an unambiguous separation of the nuclear and magnetic scattering contributions to the measured SANS intensity. The standard practice of analyzing the Q-dependence of the SANS intensity of reentrant ferromagnetic systems in terms of the expression, Lorentzian plus Lorentzian-squared, revealed that in the present case, this expression fails to adequately describe the observed variation of the magnetic component of the SANS intensity with Q, even in the reentrant state. By comparison, a model, in which spin clusters of average size ($R \approx 2$ nm) with a relatively narrow size distribution coexist with clusters of larger average size and wider size distribution, reproduces the magnetic scattering over the entire Q range at all temperatures. While the size of the smaller clusters does not change with temperature, the larger ones grow as the temperature is increased from the reentrant state at low temperatures up to the Curie temperature (T_C) through the ferromagnetic regime. The present results also strongly indicate the presence of clusters at temperatures well above T_C in the paramagnetic state.

DOI: 10.1103/PhysRevB.71.134413 PACS number(s): 75.50.Lk, 61.12.Ex

I. INTRODUCTION

There is growing experimental evidence that (i) magnetic inhomogeneity or the so-called "magnetic microstructure" is an attribute that is *inherent* to magnetic systems as different as amorphous (or crystalline) ferromagnets, nanocrystalline soft magnetic alloys, nanostructures, fine ferromagnetic particles, granular giant magnetoresistance (GMR) materials, colossal magnetoresistance (CMR) manganates, and frustrated pyrochlore oxides, and (ii) the nature of magnetic inhomogeneity basically decides the magnetic behavior of a given system.[1] Since the small-angle neutron scattering (SANS) technique is a powerful experimental tool to characterize magnetic inhomogeneity at the mesoscopic length scale of 1–1000 nm, the bulk of this evidence has come from the SANS investigations[2–12] on the aforementioned magnetic systems. Attempts to understand the origin of magnetic inhomogeneities in these systems have heavily drawn upon the existing knowledge[2–4,13–32] about the influence of spin frustration and local magnetic anisotropy on the magnetic order in the amorphous a-$Fe_{100-x}Zr_x$ ($7 \leqslant x \leqslant 12$) alloys. However, such attempts have given limited success primarily because conflicting opinions prevail about the nature and origin of magnetic inhomogeneity and about the finer details of the magnetic microstructure in a-$Fe_{100-x}Zr_x$ alloys, as elucidated below.

Magnetic susceptibility,[13,14] Mössbauer effect[15,16] and muon spin relaxation[17] data have established the following widely-accepted magnetic phase diagram for a-$Fe_{100-x}Zr_x$ alloys. Barring the alloy with $x=7$ ($x=12$), which behaves as a spin glass (conventional ferromagnet) with a well-defined freezing temperature T_f (ordering temperature T_C), the alloys with $x=8-11$ exhibit two transitions as the temperature is lowered from high temperatures; a paramagnetic (PM) to ferromagnetic (FM) transition at the Curie temperature T_C followed at a lower temperature T_{RE} by a transition from the FM state to the reentrant (RE) state. With x decreasing from $x=11$, T_{RE} increases while T_C decreases such that the $T_{RE}(x)$ and $T_C(x)$ phase transition lines meet at T_f for $x=7$. There is a general consensus that the RE state is a *mixed* state in which long-range ferromagnetic order coexists with the spin glass order but there are conflicting opinions about the exact nature of the ferromagnetic and spin glass order.

The magnetic behavior of a-$Fe_{100-x}Zr_x$ alloys has been basically understood from *four divergent* points of view. The *first* approach[14,18,19] considers the magnetic microstructure as consisting of *spin clusters* of *antiferromagnetic* (AF) Fe

spins and the *ferromagnetic* (FM) Fe–Zr *matrix* (in which these clusters are frozen in random orientations for $T \leqslant T_{RE}$) and arising from the changes in the sign of the exchange interaction due to *local* variations in the *composition* of the samples. A collinear spin structure within the clusters and matrix is, however, not supported by the Mössbauer data[15,16,20,21] which unambiguously reveal that a large percentage of magnetic moments is *noncollinear*. In agreement with the Mössbauer results, the band structure calculations[22] yield a noncollinear ferromagnetic ground state for these alloys. According to the *second* (the so-called FM cluster–FM matrix) model, proposed by Kaul *et al.*,[20,23–27] the spin system for $T \leqslant T_C$ comprises the *infinite* three-dimensional *ferromagnetic network* (matrix) and finite spin clusters (composed of a set of *noncollinear*[20] but *ferromagnetically* coupled spins), which are embedded in the *spin-canted* FM matrix[20,23,27] and frozen in random directions for $T \leqslant T_{RE}$. Contrasted with the first picture, the spatial segregation of finite FM clusters and FM matrix in this model originates from the *local* atomic *density* fluctuations. A somewhat similar model, put forward by Kiss *et al.*[28] based on the interpretation of the magnetization–magnetic field isotherms in terms of the classical theory for *interacting* superparamagnetic particles, indicates that the FM clusters occupy the entire volume of the sample. The *third* model regards the *a*-$Fe_{100-x}Zr_x$ alloys to be a "wandering axis" ferromagnet[15] in which the noncollinear magnetic moments are ferromagnetically correlated but the *local* ferromagnetic axis changes throughout the sample. The *fourth* one (the so-called transverse spin-freezing model), due to Ryan *et al.*,[15,17,29] envisages the spin system for $T \leqslant T_C$ to be composed of *ferromagnetically* correlated *longitudinal* (*z*-direction) spin components and strongly fluctuating *transverse* (*xy*) spin components; as the temperature is lowered below T_C, transverse spin components *cooperatively* freeze in random orientations in the *xy*-plane at $T = T_{RE} \approx T_{xy}$ and *coexist* with *collinear* ferromagnetic order along the *z* direction. This model essentially excludes the presence of spin clusters for it places an upper bound of 0.5% of the total spins that could form such clusters.

While the results of extensive critical phenomena studies[23–26,30–33] confirm the presence of an *infinite* FM matrix and thereby rule out the descriptions such as the "wandering axis" ferromagnet for which the spin correlation length does not diverge at $T = T_C$, there are experimental evidences for[20,23–28,30–33] (against[2–4,20,23–28,30–33]) and against[15,17,29] (for[15,17,29]) the FM cluster-FM matrix (transverse spin-freezing) model. Furthermore, from a recent polarized neutron scattering determination of the structure factor, Wildes *et al.*[34] conclude in direct contradiction with the proposal of Ryan *et al.*[15,17,29] that FeZr glasses are collinear ferromagnets with strong spin fluctuations for $T_{xy} < T < T_C$, *noncollinear* spin components are *ferromagnetically* correlated over several atomic spacings, and that the fraction of magnetic moments that are collinear with the mean ferromagnetic direction is small. This observation lends firm support[34] to the FM cluster-FM matrix model.[20,23–27] Though there is evidence for spin clusters from the SANS data,[2–4] these results cannot be regarded as conclusive for the following reasons. On the one hand, all the SANS investigations[2–4] deal with the total integrated scattering intensity which contains a sizable contribution from the nuclear scattering and on the other hand, the SANS data that extend to *Q* values (modulus of the scattering vector) as low as[4] 0.003 $Å^{-1}$ could have a large contribution due to the scattering from surface imperfections.[35]

The above considerations prompted us to undertake an extensive SANS study of amorphous $Fe_{91}Zr_9$ alloy in the wide ranges $0.003\ Å^{-1} \leqslant Q \leqslant 0.5\ Å^{-1}$ and $10\ K \leqslant T \leqslant 300\ K$ of *Q* and temperature, respectively, and to correct the SANS intensity for the scattering from surface imperfections using the results of contrast matching experiments.

II. EXPERIMENT

Amorphous ribbons of nominal composition $Fe_{91}Zr_9$ and approximately 1.5 mm wide and around 20 μm thick were obtained by rapid-quenching under Ar atmosphere (500 mbar) in a Bühler melt-spinner apparatus. The master alloy pellets, prepared in an arc-furnace, were subsequently placed inside a quartz tube with a matching end to attach a boron nitride nozzle. This nozzle was 1 mm away from the surface of the stainless steel wheel of dimensions 14 cm in diameter and 3 cm wide rotating at an angular speed of 2800 rpm. The pellets (2 g) were melted at around 1800 K prior to ribbon casting. X-ray diffraction (Cu $K\alpha$) patterns using long (1 min) integrating times per angle, taken on either faces of the ribbons, confirmed that the ribbons are in the amorphous state. The examination of the chemical composition by energy dispersive x-ray analysis in different sample areas revealed a good chemical homogeneity and an average composition of $Fe_{90.98}Zr_{9.02}$, in excellent agreement with the nominal composition.

SANS experiments were carried out in LOQ and SANS instruments at the ISIS pulsed-neutrons and Risoe DR3 reactor sources, respectively. A comparison between the data sets taken on the same sample using different instruments (time-of-flight and diffraction) constitutes a stringent test for the consistency of results. The ribbons (around 1 g) were wrapped in a thin Al foil. The selected *Q* range at the LOQ instrument was $0.006\ Å^{-1} < Q < 0.2\ Å^{-1}$. With the aim of making the results of an elaborate data analysis in the case of magnetically inhomogenous alloys more conclusive, the SANS experiments were later performed at Risoe in an extended *Q* range, $0.003\ Å^{-1} < Q < 0.5\ Å^{-1}$. Both the sets of data were taken in the zero-field and in-field conditions. At ISIS, an electromagnet ($H = 0.26$ T) was placed in the beam allowing a perpendicular geometry with respect to the long axis in the ribbon plane, and the temperature range of 10–300 K was covered using a CCR-Leybold cryostat. In Risoe, an Oxford cryostat, housing a superconducting coil, allowed a variation of temperature between 10 and 300 K and of field from $H = 0.5$ to 4 T. In this instrument, the *Q* range was achieved by selecting three different average wavelengths ($\lambda = 10$, 6, and 3 Å) and detector distances (6, 3, and 1 m). Standard corrections[36] were applied to both sets of data. The agreement between results of both instruments is excellent, as reported previously.[4] Such an agreement rules out any influence of sample mounting or the presence of

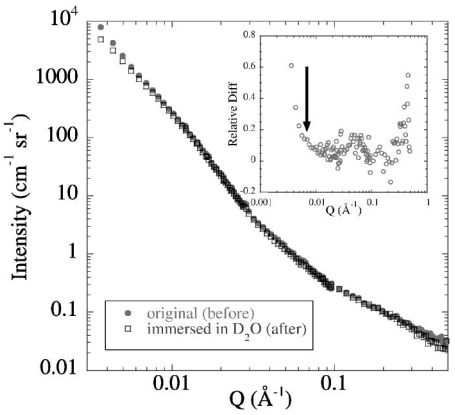

FIG. 1. SANS $I(Q)$ patterns of amorphous $Fe_{91}Zr_9$ ribbons before and after immersing them in D_2O, contained in a quartz vial. The inset shows that the difference in $I(Q)$ is negligible except for $Q<0.006$ Å^{-1} (marked with an arrow) and $Q>0.2$ Å^{-1}.

instrumental and ancillary equipment background on the signal.

To ascertain whether or not the ribbon surface has any influence on the scattered signal, a final set of experiments was performed at the SANS-Risoe instrument at room temperature. For such an experiment, we used quartz vials ($3\times0.2\times1$ cm^3) mounted on a special rig. The vials contained several ribbons (around 0.3 g) placed perpendicular to the neutron beam. Liquid D_2O (Aldrich Chemicals) was employed to obtain the best possible contrast matching.

III. DATA ANALYSIS, RESULTS, AND DISCUSSION

It is well-known that the SANS signal may have a significant contribution from the surface scattering, varying as Q^{-4} (surface states such as roughness, oxide layer, chemical composition, or surface structure) or a contribution varying as Q^{-3} due to dislocations. The former case is particularly relevant to amorphous ribbons. Previously reported SANS studies on FeZr alloys[2–4] did not take into account this effect. An efficient way of investigating such effects is to modify the scattering contrast between the sample and its surroundings by immersing the sample in liquids which have nearly the same coherent scattering length density as the sample. This is so because the small-angle scattering signal coming from the sample surface is proportional to $\langle\Delta\rho^2\rangle$, where $\Delta\rho$ is the difference in the scattering length density between the sample and the liquid. To this end, we have selected D_2O as its coherent scattering length density, $\rho=6.36\times10^{10}$ cm^{-2}, which is very close to that ($\rho=7.23\times10^{10}$ cm^{-2}) of the amorphous $Fe_{91}Zr_9$ alloy. Although it is not possible to match exactly the ρ value, the difference in the shape of the SANS patterns taken at room temperature between the ribbons in air and immersed in the contrast liquid should reflect such surface effects. Figure 1 shows a comparison between the SANS signals from the sample with and without D_2O and the relative difference between them. It is evident from the difference plot (inset of Fig. 1) that both the signals match over the entire Q range except for $Q<0.006$ Å^{-1} (marked by an arrow) and $Q>0.2$ Å^{-1}. This observation rules out any significant contribution from the sample surface in the range $0.006\ \text{Å}^{-1}\leqslant Q\leqslant0.2\ \text{Å}^{-1}$. For this reason, further analysis of the SANS data is carried out only in the range $0.006\ \text{Å}^{-1}\leqslant Q\leqslant0.1\ \text{Å}^{-1}$ where surface contributions are negligibly small. Note that the seemingly large relative difference between the sample and D_2O SANS signals for $Q>0.2$ Å^{-1} is an artifact of a background signal (emanating, in the most part, from the external cells of the detector) which is as *weak* as that due to either the sample or the sample plus D_2O. This difference signal has thus little to do with the surface effects.

The SANS signal from a magnetically concentrated material with magnetic *clusters* or *inhomogeneities* can be quite complex and hence deserves a careful analysis. Only in magnetic systems with well-defined particles or clusters (in the nanometric scale) such as bcc-Fe or Fe-oxides embedded in an insulating matrix, e.g., SiO_2 or Al_2O_3, can the SANS pattern display pronounced peaks. If the size distribution (normally taken as a log-normal) of particles is narrow and the volume fraction of particles is also small (approximately 35%), the SANS signal exhibits a peak at around $Q=0.15$ Å^{-1}, corresponding to a mean size around 3 nm.[11] In our case, the absence of peaks in the signal requires an extra effort to extract quantitative results.

The SANS intensity comprises nuclear and magnetic contributions. The nuclear contribution arises from local fluctuations in the nuclear scattering length density caused by variations in the density or chemical composition. If it is assumed that the fluctuations stem from the local variations in the chemical composition, local compositional fluctuations should give rise to Fe-rich regions which should behave as antiferromagnetic fcc-Fe clusters, with a Néel temperature around 70 K. The Néel transition is not observed in the magnetic susceptibility data and Mössbauer spectra do not reveal any antiferromagnetic spin correlations, as discussed in detail in Refs. 16, 20, 21, and 23. Hence density fluctuations are expected to be the origin of the local fluctuations in the nuclear scattering length density. The magnetic contribution, on the other hand, originates from the magnetic scattering of neutrons from fluctuations in both the orientation and the magnitude of the magnetization density, and hence *probes* the magnetic inhomogeneities in the sample. The total SANS signal depends on the magnitude Q of the scattering vector $\mathbf{Q}$ and the angle (α) between the scattering and magnetization vectors:

$$I_{TOTAL}(Q,\alpha)=I_{NUC}(Q)+I_{MAG}(Q)\sin^2\alpha \qquad (1)$$

where $I_{NUC}(Q)$ and $I_{MAG}(Q)$ are the Q-dependent nuclear and magnetic contributions. If a magnetic field H, large enough to saturate the sample (so that the directions of the vectors $\mathbf{H}$ and $\mathbf{M}$ coincide), is applied, it is possible to separate the nuclear and magnetic contributions. When $\mathbf{H}$ is parallel (*PAR*) to $\mathbf{Q}$, $\alpha=0$, and hence only the nuclear scattering $[I_{NUC}(Q)]$ contributes to the $I_{TOTAL}(Q)$. If $I(Q)$ is measured in a direction perpendicular (*PER*) to that of H, $\alpha=90°$ and hence $I_{TOTAL}(Q)=I_{NUC}(Q)+I_{MAG}(Q)$. Adopting this approach, we have applied a field as large as $H=4$ T, which lies well above the field corresponding to the technical

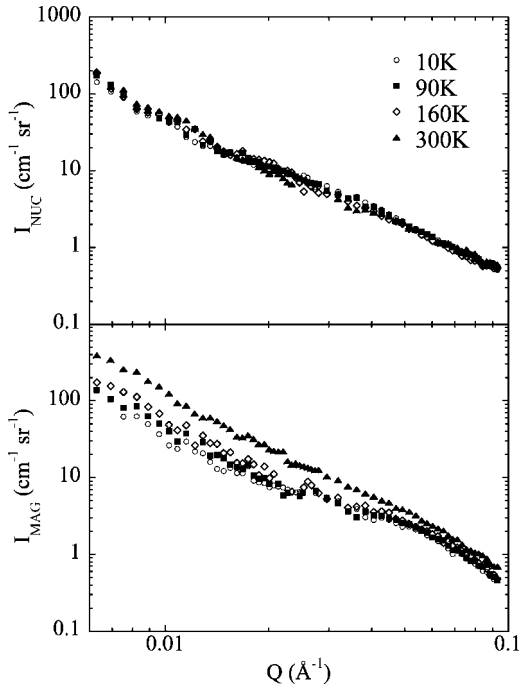

FIG. 2. $I_{MAG}(Q)=I_{PER}(Q)-I_{PAR}(Q)$ and $I_{NUC}(Q)=I_{PAR}(Q)$ at different temperatures in the reentrant 10 K, ferromagnetic (90 and 160 K), and paramagnetic 300 K regimes.

saturation[15,21,27] in the *M-H* isotherms of $Fe_{91}Zr_9$. Figure 2 shows $I_{MAG}(Q)=I_{PER}(Q)$-$I_{PAR}(Q)$ and $I_{NUC}(Q)=I_{PAR}(Q)$ at different temperatures in the reentrant (10 K), ferromagnetic (90 and 160 K), and paramagnetic (300 K) regimes.[27,37] The nuclear contribution is clearly independent of temperature at all Q values, as expected from the stability of the amorphous structure for temperatures well below the crystallization temperature ($\approx$700 K). By contrast, irrespective of Q, the magnetic contribution increases with temperature due to the thermally induced changes in the orientation and/or magnitude of the magnetization density. In addition, $I_{MAG}(Q)$ exhibits broad humps at $Q\approx 0.01$ and 0.05 Å^{-1}, particularly for $T<T_C$, indicating the presence of magnetic inhomogeneities.

To determine the influence of the field on the magnetic contribution, $I_{NUC}(Q)$ has been subtracted from the SANS intensity measured at $H=0$, 0.26, 0.5, and 4 T along the direction perpendicular to the field. Figure 3 depicts the thermal variation of the magnetic component of the scattering intensity, I_{MAG}, for the two selected Q values (0.01 and 0.08 Å^{-1}) at the above-mentioned field values. As the temperature is raised from 10 K, I_{MAG} at $H=0$ decreases initially and goes through a *peak* at 205 K for both the Q values but $I_{MAG}(Q=0.01$ Å$^{-1})$ is at least *two orders of magnitude larger* than $I_{MAG}(Q=0.08$ Å$^{-1})$ at all temperatures. For the lower Q value, the magnetic scattering intensity increases monotonously with temperature at *finite* fields. At any given temperature, the intensity reduces drastically in fields as small as 0.26 T from its value at $H=0$ such that the suppression in I_{MAG} increases as the temperature is lowered below $\sim$120 K and the peak in $I_{MAG}(T)$ disappears (by comparison, the progressive suppression with field for $H>0.26$ T is extremely small). By contrast, the reduction in $I_{MAG}(T)$ at Q

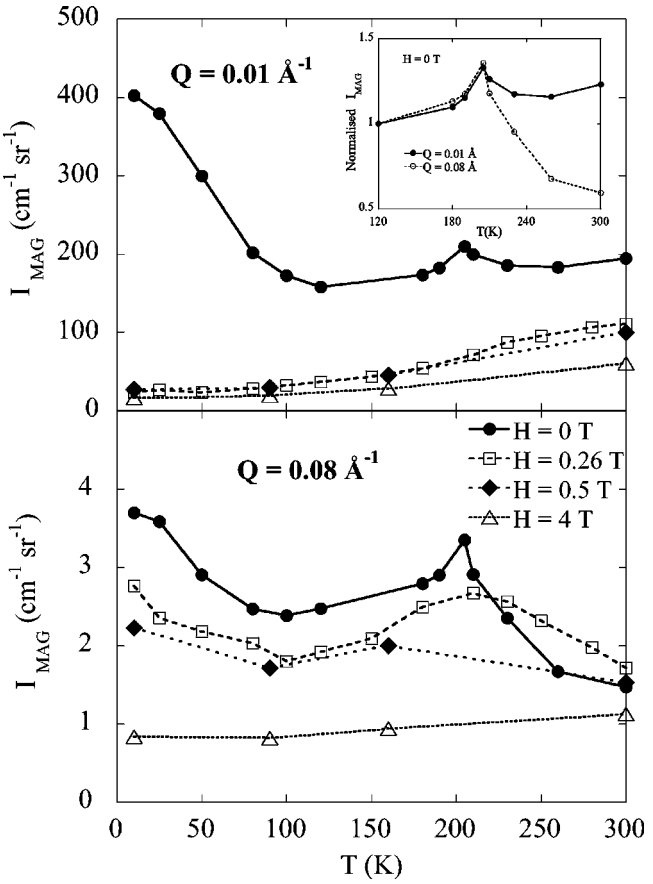

FIG. 3. Thermal variation of the magnetic component of the scattering intensity, I_{MAG}, for the two selected Q values (0.01 and 0.08 Å^{-1}) at $H=0$, 0.26, 0.5, and 4 T. A peak, visible at $T\approx T_C$, is progressively smeared out by increasing the applied field strength. The inset shows $I_{MAG}(T)$, normalized to its value at $T=120$ K, for $Q=0.01$ Å^{-1} (closed circles) and $Q=0.08$ Å^{-1} (open circles).

$=0.08$ Å^{-1} with field is not as drastic as at $Q=0.01$ Å^{-1}. In order to bring out clearly the effect of the variation in Q, the inset of Fig. 3 compares $I_{MAG}(T)/I_{MAG}(T=120$ K) at $H=0$ for the above Q values. The peak in $I_{MAG}(T)$ at[26,33,37] $T\approx T_C=210$ K, arising from the critical fluctuations of spontaneous magnetization, is sharper at the larger Q value. Contrasted with this behavior, for a conventional ferromagnet (i.e., a *homogeneous* spin system with *long-range* ferromagnetic order), I_{MAG} is *independent* of temperature for $T<T_C$ and the peak at T_C becomes more and more pronounced as Q decreases. A sharp rise in the magnetic scattering intensity for $T<120$ K and a higher value for $I_{MAG}(T)/I_{MAG}(T=120$ K) at $T>T_C$ for $Q=0.01$ Å^{-1} is thus a manifestation of the presence of an extra contribution coming from the regions differing from the ferromagnetic matrix in the orientation and/or magnitude of the magnetization density (alternatively, from the magnetic inhomogeneities) and persisting to temperatures well above T_C. Moreover, a considerably large magnitude of I_{MAG} at $Q=0.01$ Å^{-1} in the absence of the field and its extreme sensitivity to the field strongly indicate that many such regions with a wide size distribution are present in the amorphous *a*-$Fe_{91}Zr_9$ alloy. This inference follows from the fact that the magnetic inhomogeneities with size

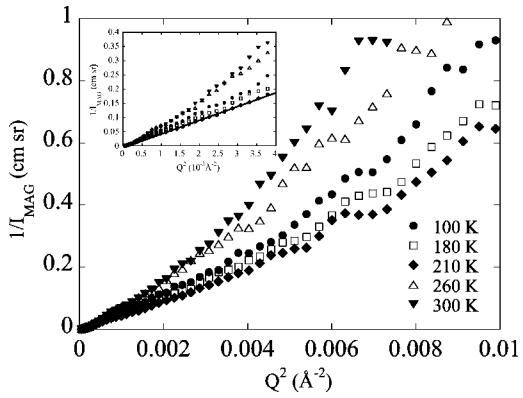

FIG. 4. $1/I_{MAG}(Q)$ vs Q^2 at different temperatures. Deviations from the true Lorentzian behavior at $Q>Q^*$ are clearly visible. Inset demonstrates that $1/I_{MAG}(Q)$ varies linearly with Q^2 for $Q^2 \leqslant 0.004$ Å^{-2} at $T=T_C$ where the least-squares-fitted straight line passes through the origin when extrapolated to $Q=0$.

larger than the length scale suggested by $Q=0.08$ Å^{-1} would have escaped detection in the I_{MAG} signal measured at $Q=0.08$ Å^{-1}. That the field progressively smears out the peak in $I_{MAG}(T)$ at T_C is a consequence of the suppression of critical fluctuations by H.

In a conventional ferromagnet, the SANS magnetic intensity is directly proportional to the spin-spin correlation function which follows an Ornstein-Zernike law in the paramagnetic regime. In accordance with this law, the magnetic scattering intensity is described by a Lorentzian. For temperatures below T_C, the rotational symmetry of the spins is spontaneously broken and hence $I_{MAG}(Q)$ is described by two Lorentzians corresponding to longitudinal and transverse critical spin fluctuations.[38] In ferromagnetic systems which exhibit a reentrant behavior at low temperatures, it is customary to fit the magnetic scattering contribution to an expression:

$$I_{MAG}(Q) = \frac{A}{Q^2+\kappa_1^2} + \frac{B}{(Q^2+\kappa_2^2)^2} \tag{2}$$

where $\kappa=1/\xi$ and ξ is the spin-spin correlation length. This is so because in the reentrant state, long-range ferromagnetic order coexists with the spin-glass order, so that in addition to a Lorentzian term (which describes the ferromagnetic contribution), Eq. (2) includes a Lorentzian squared term that accounts for the supplementary contribution arising from the spins constituting the spin-glass state.

To ascertain whether or not the *pure* magnetic signal $I_{MAG}(Q)$ at $H=0$ is described by a Lorentzian, $1/I_{MAG}(Q)$ is plotted against Q^2 at different but fixed values of temperature in Fig. 4. Deviations from the true Lorentzian behavior are apparent for $Q>Q^*$ and Q^* is *temperature-dependent*. However, the data over a certain Q range for $Q>Q^*$ can be described by another Lorentzian. As $T\rightarrow T_C$, the variation of $1/I_{MAG}(Q)$ with Q^2 at low Q becomes linear over a wider Q range and the value of κ decreases so much so that $\kappa=0$ (i.e., the spin-spin correlation length ξ *diverges*) at $T=T_C=210$ K (the inset of Fig. 4). These observations support the existence of at least two different length scales. At larger (shorter) length scales, i.e., for $Q<Q^*$ ($Q>Q^*$), the magnetic behavior is that of a conventional ferromagnet (correlated spin regions).

Since the data cannot be described by a single Lorentzian over the entire Q range and the sample in question exhibits magnetic irreversibility (i.e., a bifurcation between the "field-cooled" and the "zero-field-cooled" thermomagnetic curves for $T\leqslant T_{RE}$) characteristic[18,20,27,37] of reentrant ferromagnetic systems, the next step is to test whether Eq. (2) reproduces the observed $I_{MAG}(Q)$. We have performed this analysis on two sets of $I_{MAG}(Q)$ data taken at different temperatures in the absence ($H=0$) and presence ($H=4$ T) of the magnetic field. In Fig. 5, $I_{MAG}(Q)$ data are shown along with the best fits (dashed lines), based on Eq. (2), for selected temperatures 10 K ($<T_{RE}$), 90–100 K ($\approx T_{RE}$), 160–180 K ($<T_C$), and 300 K ($>T_C$). The calculated variations reproduce the observed $I_{MAG}(Q)$ only for $Q<0.02$ Å^{-1} and deviate appreciably from the data at all temperatures at higher Q values and hence Eq. (2) does not form an adequate description of $I_{MAG}(Q)$ in $Fe_{91}Zr_9$ even in the reentrant state.

A strong indication from the data presented in Figs. 3 and 4 for the existence of different length scales over which the spins seem to be correlated, besides the infinite ferromagnetic matrix at $T<T_C$, prompted us to take recourse to a model, normally used to describe the $I_{MAG}(Q)$ signal from single-domain magnetic nanoparticles,[39] suitably modified to include an extra contribution from particles of another size. Starting from the expression for the pure magnetic scattering cross section:

$$\left(\frac{d\sigma}{d\Omega}\right)_{MAG} = \left(\frac{d\sigma}{d\Omega}\right)_{\perp} - \left(\frac{d\sigma}{d\Omega}\right)_{\parallel} = N_p V_p^2 \Delta\rho_{MAG}^2 \sin^2\alpha F_p^2(Q) S(Q), \tag{3}$$

where N_p is the number of particles in the sample, V_p is the volume of these particles, $F_p(Q)$ their form factor, and $\Delta\rho_{MAG}$ is the magnetic contrast of the particles with respect to the matrix. The latter quantity is proportional to the magnetic moment per atomic volume. α is the angle between the scattering and the particle-magnetization directions and $S(Q)$ is the structure factor corresponding to the particles. Since there is no evidence of a peak in the $I_{MAG}(Q)$, reflecting the polydispersity of such particles in the matrix in our case, we set $S(Q)=1$ in the range of Q values covered in the present experiments.

The form factor $F_p(Q)$ (normalized to 1) for spherical particles of radius R is given by the expression

$$F_p(Q) = 3\frac{\sin(QR) - QR\cos(QR)}{Q^3R^3}. \tag{4}$$

To take into account particles of two different average sizes, we include two log-normal distributions of particle sizes. The total magnetic scattering cross section can thus be written as

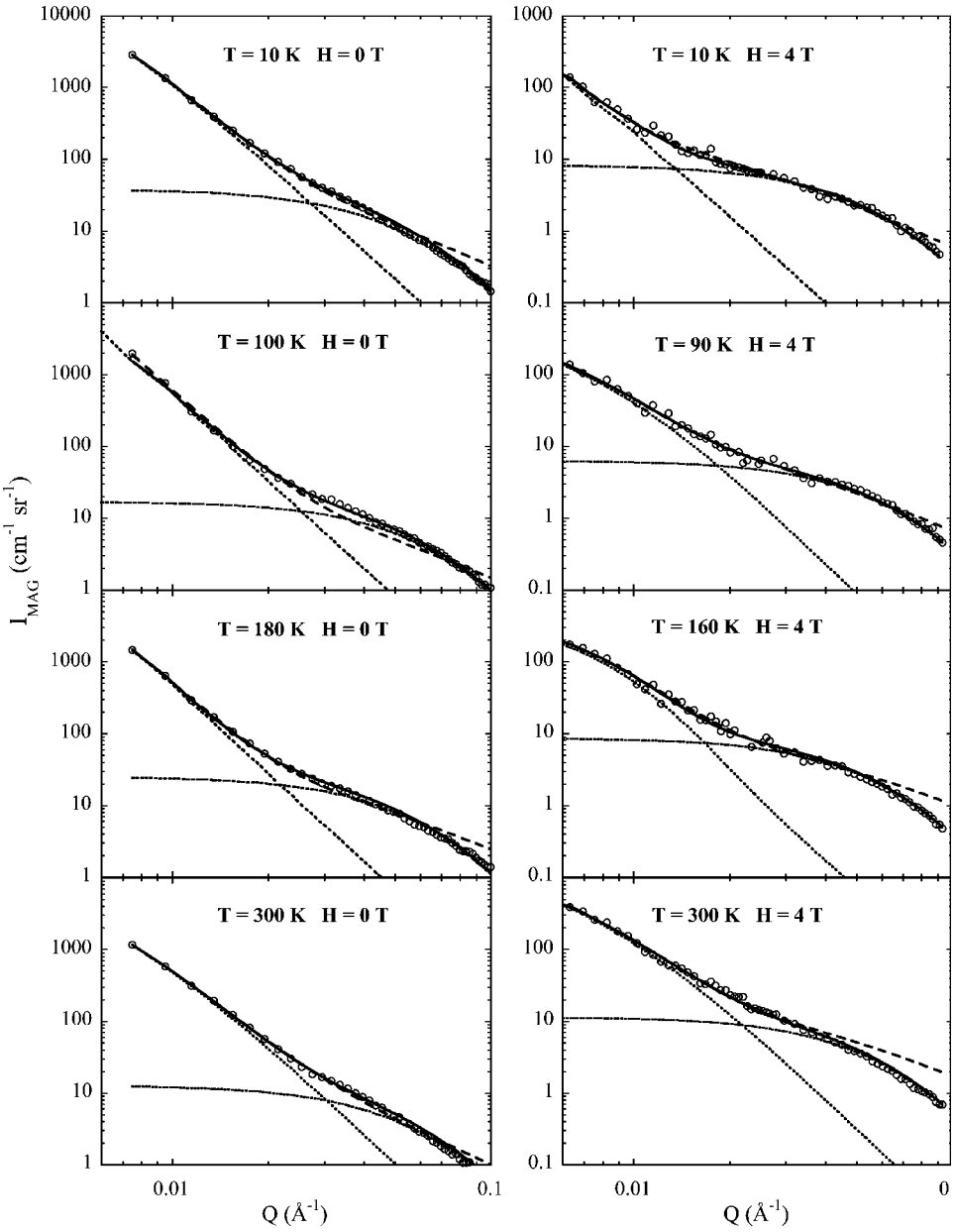

FIG. 5. $I_{MAG}(Q)$ data and the best fits (dashed curves), based on Eq. (2), for selected temperatures 10 K ($<T_{RE}$), 90–100 K ($\approx T_{RE}$), 160–180 K ($<T_C$), and 300 K ($<T_C$). The calculated variations reproduce the observed $I_{MAG}(Q)$ only for $Q<0.02$ Å^{-1} and deviate appreciably from the data at all temperatures. This is clear-cut evidence of the failure of the Lorentzian plus Lorentzian square expression to fit the data in the entire Q range. Theoretical fits (continuous curves), based on Eq. (5), to the $I_{MAG}(Q)$ data at $H=0$ (left) and $H=4$ T (right) are also shown for comparison. Continuous curves, using Eq. (5), are noticed to closely reproduce the observed $I_{MAG}(Q)$ over the entire Q range at all temperatures. This figure also depicts the individual variations with Q of the contributions to $I_{MAG}(Q)$ due to the two terms in Eq. (5) by the dotted curves.

$$\frac{1}{V}\left(\frac{d\sigma}{d\Omega}\right)_{MAG} = \Delta\rho_{mag}^2 \sin^2\alpha \left[f_{p1} \frac{\int_0^\infty g_1(R) V_1{}^2(R) F^2(Q,R) dR}{\int_0^\infty g_1(R) V_1(R) dR} + f_{p2} \frac{\int_0^\infty g_2(R) V_2{}^2(R) F^2(Q,R) dR}{\int_0^\infty g_2(R) V_2(R) dR} \right], \quad (5)$$

where V is the sample volume, f_p the volume fraction of particles of each distribution in the sample, and $g(R)$ is the log-normal size distribution.

In Fig. 5 the optimum theoretical fits, based on Eq. (5), to the $I_{MAG}(Q)$ data at $H=0$ (left) and $H=4$ T (right) are denoted by continuous curves. Note that in these fits the factor $\sin^2\alpha$ is set equal to 0.5 and 1.0 for the cases $H=0$ and 4 T, respectively, for the following reason. In the absence of the magnetic field, magnetization vectors of the particles, *confined* to the *ribbon plane* by the *shape anisotropy*, have directions *isotropic* in space since the in-plane anisotropy is extremely small.[24,25] Consequently, the spatial average of $\sin^2\alpha=0.5$. On the other hand, at $H=4$ T, the sample magnetization is nearly saturated so that the magnetization is pointing in the field direction and thus for the perpendicular geometry, $\alpha=90°$ [for details, see the paragraph below Eq. (1)] and hence $\sin^2\alpha=1$. An excellent agreement between the experiment and theory over the entire Q range is evident at all temperatures and at fields $H=0$ and 4 T. Figure 5 also depicts the individual variations with Q of the contributions to $I_{MAG}(Q)$ due to the two terms in Eq. (5) by the dotted curves. The corresponding log-normal distributions of the particle sizes (correlated spin regions in the present case) are

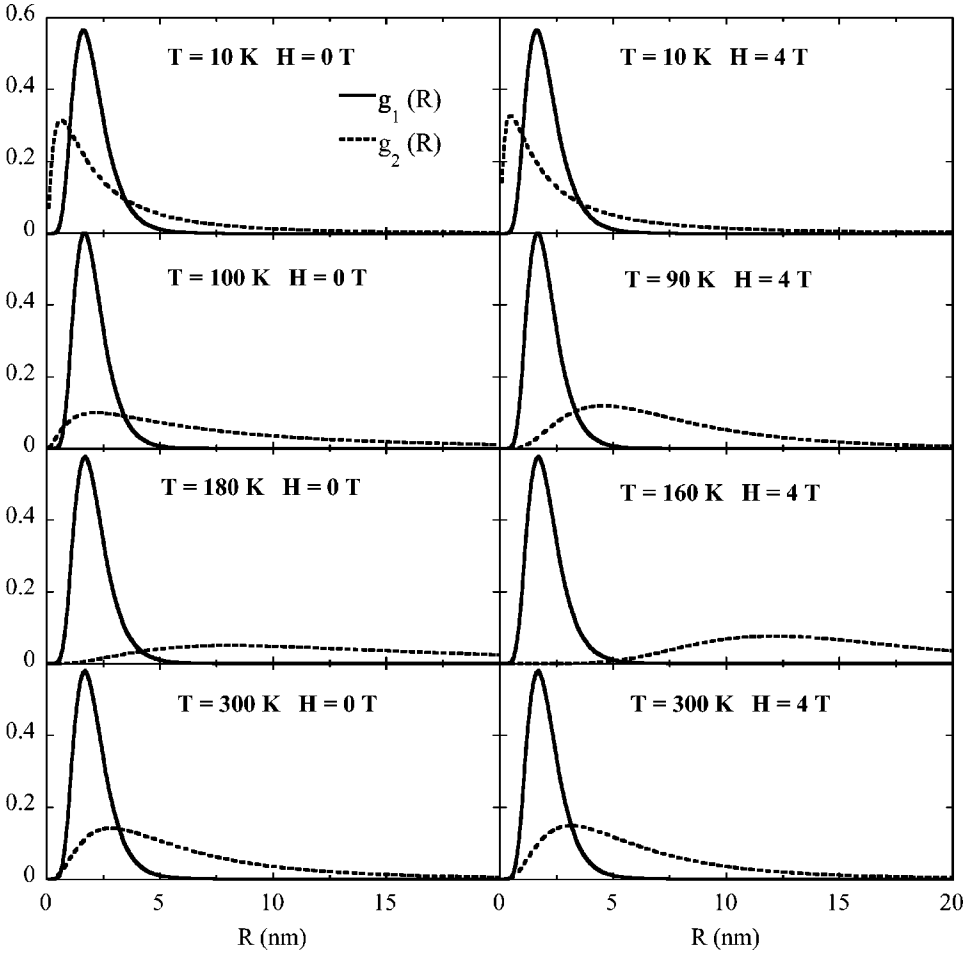

FIG. 6. Log-normal distributions of the cluster sizes (correlated spin regions in the present case) corresponding to the best fits, based on Eq. (5), displayed in Fig. 5 for $H=0$ and 4 T. The clusters of smaller average size do not vary in size with temperature as opposed to the clusters of longer spin correlation length that exhibit temperature-induced growth.

displayed in Fig. 6. It is evident from this figure that there are two kinds of correlated spin regions. The first type has an average size of $\overline{R_1}\sim 2$ nm and a narrow size distribution, with the property that both the average size as well as the size distribution are essentially *independent* of temperature from 10 to 300 K. By contrast, the second type has a similar average size $\overline{R_2}\cong\overline{R_1}$ but a much wider size distribution at $T=10$ K and as the temperature is raised through T_C, $\overline{R_2}$ increases and the size distribution progressively broadens further until $T\approx T_C$ and then $\overline{R_2}$ decreases and the size distribution narrows down for temperatures above T_C. The individual contributions made by the two terms, appearing in Eq. (5), to $I_{MAG}(Q)$ (i.e., the dotted curves in Fig. 5), when viewed against the information provided by Fig. 6 about the type of correlated spin regions (henceforth referred to as finite spin clusters) present, reveal that the magnetic scattering by spin clusters of smaller (bigger) size with narrower (broader) size distribution completely accounts for $I_{MAG}(Q)$ for $Q>0.02$ Å^{-1} ($Q<0.02$ Å^{-1}). This inference conforms very well with that drawn earlier from the data presented in Fig. 3. It is also amply clear that a single cluster size (log-normal) distribution cannot describe $I_{MAG}(Q)$ over the entire Q range. Another important observation (Fig. 6) is that the magnetic field does not seem to have any discernible influence on the spin cluster size distributions at different temperatures and hence on the temperature-induced growth of the larger spin clusters. Thus the effect of field is to orient the spin clusters towards its own direction and thereby reduce the magnetic contrast of the spin clusters with respect to the ferromagnetic matrix. Consequently, the magnetic scattering intensity is considerably reduced in the presence of the field.

The results of an elaborate analysis of the SANS taken over a wide range of Q on *a*-$Fe_{91}Zr_9$ provide strong evidence for *two kinds* of spin clusters that *coexist* with the *infinite* ferromagnetic matrix for $T<T_C$ and distinguish themselves in the way they respond to the variations in temperature; while the temperature has practically no influence on the average size and size distribution of one type of spin clusters, it induces growth in both the average size and size distribution of the spin clusters of the other type until the sample warms up to T_C and then disintegrates/disorders them for $T>T_C$ with the result that the average size reduces and the size distribution narrows down. Next, we attempt an interpretation of these observations in terms of the models proposed in the literature and described in the Introduction (Sec. I). While the presence of an infinite ferromagnetic matrix for $T<T_C$ and hence the divergence of the spin-spin correlation length ξ at $T=T_C$ (inset of Fig. 4) rules out the descriptions such as the "wandering-axis" ferromagnet,[15] since in such a ferromagnet ξ *does not diverge* at $T=T_C$, the presence of clusters, and that too in a great proportion, is in direct contradiction with the transverse spin-freezing model[15,17,29] because it considers the spin system to be magnetically *homogeneous* even on the microscopic scale. By comparison, the

coexistence of finite spin clusters with the infinite ferromagnetic (FM) matrix finds a natural place in the so-called FM cluster–FM matrix model,[20,23–27] which envisages the spin system for $T \leqslant T_C$ to be composed of the *infinite* three-dimensional *ferromagnetic network* (matrix) and finite spin clusters (composed of a set of *noncollinear*[20] but *ferromagnetically* coupled spins), which are embedded in, but either *partially* or *completely isolated* from, the FM matrix by *zones of frustrated spins* surrounding the finite clusters. According to this model, the exchange interaction between spins in the FM matrix weakens as $T \rightarrow T_C$ while the FM coupling between the spins within the finite clusters is still quite strong due to the higher Curie temperature for the clusters. As a consequence, the spins of the clusters that are *partially isolated* from, and hence weakly interact with, not only the FM matrix but also the neighboring clusters (the so-called strongly interacting clusters) can grow in size with temperature through two mechanisms. In one such mechanism, they can merge together because of the strong coupling between the neighboring clusters to form a bigger cluster. In the other, the cluster spins are able to polarize an increased number of spins originally belonging to the FM matrix via direct exchange interactions,[40] and hence the clusters grow in size at the expense of the spins contained in the FM matrix. However, the temperatures in excess of T_C disorder not only the FM matrix but also the clusters and hence the cluster size decreases for temperatures above T_C. On the other hand, none of the above-mentioned mechanisms can induce growth in the clusters which are *completely isolated* (so far as the direct exchange interactions are concerned) from the FM matrix and also from other clusters (the so-called noninteracting clusters). Note that this decoupling is similar to the one observed in FeZrCuB alloys, where minuscule quantities of Fe grains are embedded in an amorphous matrix.[41] Thus such clusters cannot grow in size with increasing temperatures, in agreement with the present observations. The net result of the temperature-induced cluster growth and the existence of many isolated clusters is that a *major* fraction of total spins resides in the *finite* clusters for temperatures in the vicinity of T_C. The growth process resulting in an increasing presence of large clusters would naturally enhance long-range Ruderman-Kittel-Kasuya-Yoshida and dipolar interactions between clusters because of the large magnitude of the cluster moments.

If the spins within the clusters (matrix) were antiferromagnetically (ferromagnetically) coupled, as considered in the antiferromagnetic (AF) spin cluster-FM matrix model,[14,18,19] it is not easy for the AF cluster spins to polarize the FM matrix spins and thereby grow in size with increasing temperature because of a much higher energy cost involved in this process. Thus our observations do not support such a model, although it should be noted that the SANS technique cannot distinguish between the canted or collinear configuration of the cluster spins.

The temperature-induced growth of the finite FM spin clusters in a-$Fe_{90+x}Zr_{10-x}$ alloys has also been previously inferred from Mössbauer,[20] ferromagnetic resonance,[24,25] and bulk magnetization[23,26] results. Unlike these techniques, the SANS data provides direct evidence for the presence of clusters in a FM matrix. Accordingly, this type of data analysis could be extended to SANS data on other magnetically heterogeneous systems of current interest such as ultrasoft nanocrystalline magnets, interacting fine-particles, and CMR-oxides, to name a few.

IV. SUMMARY AND CONCLUSIONS

We have performed in-field and zero-field SANS measurements at different temperatures between 10 and 300 K in an archetypal reentrant amorphous ferromagnet $Fe_{91}Zr_9$. Contrast matching experiments before and after immersing the alloy ribbons in deuterium oxide have also been carried out at room temperature to ascertain the Q range in which the surface scattering contribution becomes important. The results of the latter experiments show that only for $Q < 0.006$ Å^{-1} the surface effect tends to be important.

An unambiguous separation of the magnetic and nuclear scattering contributions to the measured SANS signal has been made by applying a field as high as $H=4$ T, larger than that corresponding to the technical saturation in the magnetization of the sample. Although definite indications of the presence of two different contributions stemming from spins correlated over two different length scales are observed, the magnetic contribution cannot be explained over the entire Q range using the standard approach of fitting the data to Lorentzian + Lorentzian squared contributions. By contrast, an alternative analysis that takes into account the contributions from spherical clusters of two different spin correlation length distributions leads to an excellent agreement with the experimental data. The temperature variation of the SANS patterns reveals the existence of small (around 2 nm in radius) clusters that do not change in size with temperature, and the larger clusters with a thermally induced growth from the reentrant regime at low temperatures ($T < 50$ K) up to the Curie temperature through the ferromagnetic regime. This growth is due to the coalescence of neighboring spin clusters into bigger ones and also by the polarization of nearby spins, originally belonging to the ferromagnetic matrix. There are clear indications that the spin clusters persist to temperature well above T_C into the paramagnetic state.

ACKNOWLEDGMENTS

The authors thank Professor O. V. Nielsen for permitting the use of his melt-spinning setup, the MEC program (SAB2001-0086) for supporting the sabbatical stay of Professor S. N. Kaul at the Universidad de Cantabria, and Dr. I. Mirebeau (LLB-Saclay) for helpful comments on the data analysis. This work has been funded by CICYT MAT2002-04178-CO4.

*On sabbatical leave from School of Physics, University of Hyderabad, Hyderabad 500046, India.
†Present address: Department of Chemistry, University of Aarhus, Langelandsgade 140, DK-8000 Aarhus, Denmark.

[1] R. C. O'Handley, *Modern Magnetic Materials: Principles and Applications* (Wiley, New York, 2000).
[2] J. J. Rhyne, R. W. Erwin, J. A. Fernández-Baca, and G. E. Fish, J. Appl. Phys. **63**, 4080 (1988).
[3] K. Mergia, S. Messoloras, G. Nicolaides, D. Niarchos, and R. J. Stewart, J. Appl. Phys. **76**, 6380 (1994).
[4] L. Fernández Barquín, J. C. Gómez Sal, S. N. Kaul, J. M. Barandiarán, P. Gorria, J. S. Pedersen, and R. Heenan, J. Appl. Phys. **79**, 5146 (1996).
[5] B. Schönfeld, O. Paris, G. Kostorz, and J. S. Pedersen, J. Phys.: Condens. Matter **10**, 8395 (1998).
[6] H. N. Frase, B. Fultz, S. Spooner, and J. L. Robertson, J. Appl. Phys. **85**, 7097 (1999).
[7] A. Danzig, A. Wiedenmann, and N. Mattern, J. Phys.: Condens. Matter **10**, 5267 (1998).
[8] A. Wiedenmann, U. Lembke, A. Hoell, R. Müller, and W. Schüppel, Nanostruct. Mater. **12**, 601 (1999).
[9] J. Weissmüller, A. Michels, J. G. Barker, A. Weidenmann, U. Erb, and R. D. Shull, Phys. Rev. B **63**, 214414 (2001); A. Michels, R. N. Viswanath, J. G. Barker, R. Birringer, and J. Weissmüller, Phys. Rev. Lett. **91**, 267204 (2003).
[10] M. B. Fernández van Raap, L. M. Socolovsky, F. H. Sánchez, and I. L. Torriani, J. Phys.: Condens. Matter **14**, 857 (2002).
[11] C. Bellouard, I. Mirebeau, and M. Hennion, Phys. Rev. B **53**, 5570 (1996).
[12] J. E. Greedan, N. P. Raju, A. Maignan, Ch. Simon, J. S. Pedersen, A. M. Niraimathi, E. Gmelin, and M. A. Subramanian, Phys. Rev. B **54**, 7189 (1996).
[13] D. A. Read, T. Moyo, and G. C. Hallam, J. Magn. Magn. Mater. **44**, 279 (1984).
[14] N. Saito, H. Hiroyoshi, K. Fukamichi, and Y. Nakagawa, J. Phys. F: Met. Phys. **16**, 911 (1986).
[15] D. H. Ryan, J. M. D. Coey, E. Batalla, Z. Altounian, and J. O. Ström-Olsen, Phys. Rev. B **35**, 8630 (1987); H. Ren and D. H. Ryan, *ibid.* **51**, 15 885 (1995).
[16] D. Kaptas, T. Kemény, L. F. Kiss, J. Balogh, L. Gránásy, and I. Vincze, Phys. Rev. B **46**, 6600 (1992); J. Non-Cryst. Solids **156-158**, 336 (1993).
[17] J. Van Lierop and D. H. Ryan, Phys. Rev. Lett. **86**, 4390 (2000); D. H. Ryan, J. Van Lierop, M. E. Pumerol, M. Roseman, and J. M. Cadogan, J. Appl. Phys. **89**, 7039 (2001).
[18] H. Hiroyoshi and K. Fukamichi, J. Appl. Phys. **53**, 2226 (1982).
[19] D. A. Read, G. C. Hallam, and M. Chirwa, J. Magn. Magn. Mater. **82**, 83 (1989).
[20] S. N. Kaul, V. Siruguri, and G. Chandra, Phys. Rev. B **45**, 12 343 (1992); S. N. Kaul, C. Bansal, T. Kumaran, and M. Havalgi, *ibid.* **38**, 9248 (1988).
[21] I. Vincze, D. Kaptás, T. Kemény, L. F. Kiss, and J. Balogh, Phys. Rev. Lett. **73**, 496 (1994).
[22] R. Lorentz and J. Hafner, J. Magn. Magn. Mater. **139**, 209 (1995).
[23] S. N. Kaul, J. Appl. Phys. **61**, 451 (1987); J. Phys. F: Met. Phys. **18**, 2089 (1988); J. Phys.: Condens. Matter **3**, 4027 (1991).
[24] S. N. Kaul and Ch. V. Mohan, J. Phys.: Condens. Matter **3**, 2703 (1991); S. N. Kaul and V. Siruguri, *ibid.* **4**, 505 (1992).
[25] S. N. Kaul and P. D. Babu, Phys. Rev. B **45**, 295 (1992); V. Siruguri and S. N. Kaul, J. Phys.: Condens. Matter **8**, 4567 (1996).
[26] P. D. Babu and S. N. Kaul, J. Phys.: Condens. Matter **9**, 7189 (1997).
[27] S. N. Kaul and P. D. Babu, J. Phys.: Condens. Matter **10**, 1563 (1998); S. N. Kaul and S. Srinath, *ibid.* **10**, 11067 (1998).
[28] L. F. Kiss, T. Kemény, I. Vincze, and L. Gránásy, J. Magn. Magn. Mater. **135**, 161 (1994).
[29] D. H. Ryan, J. M. Cadogan, and S. J. Kennedy, J. Appl. Phys. **79**, 6161 (1996); D. H. Ryan, J. M. Cadogan, and J. Van Lierop, Phys. Rev. B **61**, 6816 (2000); D. H. Ryan, A. D. Beath, E. McCalla, J. Van Lierop, and J. M. Cadogan, *ibid.* **67**, 104404 (2003).
[30] H. Ma, H. P. Kunkel, and G. Williams, J. Phys.: Condens. Matter **3**, 5563 (1991).
[31] R. Reisser, M. Fähnle, and H. Kronmüller, J. Magn. Magn. Mater. **75**, 45 (1988); R. Reisser, M. Seeger, M. Fähnle, and H. Kronmüller, *ibid.* **110**, 32 (1992).
[32] A. Perumal, V. Srinivas, A. Dhar, V. V. Rao, and R. A. Dunlap, Phys. Status Solidi A **178**, 783 (2000); A. Perumal, Pramana J. Phys. **56**, 569 (2001).
[33] K. Balakrishnan and S. N. Kaul, Phys. Rev. B **65**, 134412 (2002).
[34] A. R. Wildes, J. R. Stewart, N. Cowlam, S. Al-Heniti, L. F. Kiss, and T. Kemeny, J. Phys.: Condens. Matter **15**, 675 (2003).
[35] B. Rodmacq, Ph. Mangin, and A. Chamberod, Phys. Rev. B **30**, 6188 (1984).
[36] J. S. Pedersen, J. Phys. (Paris), Colloq. C8 **3**, 491 (1993).
[37] L. Fernández Barquín, J. C. Gómez Sal, P. Gorria, J. S. Garitaonandia, and J. M. Barandiarán, Eur. Phys. J. B **35**, 3 (2003).
[38] Ph. Mangin, D. Boumazouza, B. George, J. J. Rhyne, and R. W. Erwin, Phys. Rev. B **40**, 11 123 (1989); G. Aeppli, S. M. Shapiro, R. J. Birgeneau, and H. S. Chen, Phys. Rev. B **28**, 5160 (1983).
[39] M. H. Mathon and C. H. de Novion, J. Phys. IV **9** (1), 127 (1999); J. Henry, M. H. Mathon, and P. Jung, J. Nucl. Mater. **318**, 249 (2003).
[40] A. Hernando, I. Navarro, and P. Gorria, Phys. Rev. B **51**, 3281 (1995).
[41] J. S. Garitaonandia, P. Gorria, L. Fernández Barquín, and J. M. Barandiarán, Phys. Rev. B **61**, 6150 (2000).